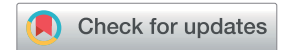
RSC Advances



PAPER

View Article Online
View Journal | View Issue



Cite this: RSC Adv., 2023, 13, 31595

Synthesis and evaluation of potent (iso)ellipticinebased inhibitors of MYLK4 accessed *via* expeditious synthesis from isoquinolin-5-ol[†]

Szu Lee,‡^a Min-Wu Chao,‡^{bcd} Yi-Wen Wu,^e Chia-Min Hsu,^e Tony Eight Lin,^{ef} Kai-Cheng Hsu,^{efghi} Shiow-Lin Pan^{efghi} and Hsueh-Yun Lee ¹ **Dane **In The State of t

The $K_2S_2O_8$ -mediated generation of p-iminoquinone contributed to the regioselective substitution of isoquinolin-5,8-dione. This hydroxyl group-guided substitution was also applied to selected heterocycles and addressed the regioselectivity issue of quinones. This study has provided an expeditious pathway from isoquinolin-5-ol (5) to ellipticine (1) and isoellipticine (2), which benefits the comprehensive comparison of their activity. Compounds 1 and 2 displayed marked MYLK4 inhibitory activity with IC₅₀ values of 7.1 and 6.1 nM, respectively. In the cellular activity of AML cells (MV-4-11 and MOLM-13), compound 1 showed better AML activity than compound 2.

Received 27th September 2023 Accepted 23rd October 2023

DOI: 10.1039/d3ra06600b

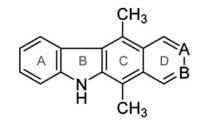
rsc.li/rsc-advances

Introduction

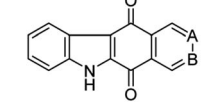
The pyrido[4,3-*b*]carbazole alkaloid ellipticine (1) was isolated by Goodwin *et al.*¹ in 1959 from *Ochrosia elliptica* Labill. Ellipticine and its relevant analogues were reported to exhibit anticancer activity, possibly by DNA intercalation and inhibition of topoisomerase II.²⁻⁴ Because of its biological activity, it was of interest for researchers to develop synthetic approaches to ellipticine. The approaches are simply summarized into four methodologies according to late-stage ring formation of the B-, C-, D- and B/C-rings. The B-ring can be constructed from an aryl

triazene^{5,6} with a Pd-catalyzed cross-dehydrogenative coupling reaction.⁷ Much efforts has been devoted to the formation of the C-ring of ellipticine through a Diels–Alder reaction between furo[3,4-*b*]indole and 3,4-pyridyne^{8,9} or between pyrano[3,4-*b*] indol-3-one and pyridyltriazene.¹⁰ The lateral D-ring can be built from 3-formyl-1,4-dimethylcarbazole by a Pomeranz–Fritsch isoquinoline synthesis.¹¹⁻¹³ Differding *et al.* reported the intramolecular Diels–Alder cycloaddition of vinylketenimine, which assembled the B and C rings of ellipticine simultaneously.¹⁴ In addition, Pedersen showed that the B/C rings of ellipticine could also be constructed by an imidoyl radical cascade reaction (Fig. 1).¹⁵

In addition to the methodologies cited above, ellipticine quinone (3) is considered to be a precursor of ellipticine, to which it could be converted by reaction of the carbonyl groups with methyl lithium followed by treatment with sodium borohydride. Ellipticine quinone (3) was obtained by a tandem directed metalation reaction between indole-3-carboxaldehyde and *N,N*-diethylisonicotinamide, Friedel–Crafts hydroxyalkylation of the resulting ethyl indole-3-carboxylate followed by oxidation and *ortho*-lithiation, or lead tetraacetatemediated oxidative rearrangement of an acyl hydrazone



1: ellipticine (A = N; B = C) 2: isoellipticine (A = C; B = N)



3: ellipticine quinone (A = N; B = C)4: isoellipticine quinone (A = C; B = N)

Fig. 1 Structures of (iso)ellipticine (1 and 2) and (iso)ellipticine quinone (3 and 4).

[&]quot;School of Pharmacy, College of Pharmacy, Taipei Medical University, Taiwan. E-mail: hyl@tmu.edu.tw; Tel: +886-2-7361661

^bSchool of Medicine, College of Medicine, National Sun Yat-sen University, Kaohsiung, Taiwan

^cInstitute of Biopharmaceutical Sciences, College of Medicine, National Sun Yat-sen University, Kaohsiung, Taiwan

^aThe Doctoral Program of Clinical and Experimental Medicine, College of Medicine, National Sun Yat-sen University, Kaohsiung, Taiwan

^eGraduate Institute of Cancer Biology and Drug Discovery, College of Medical Science and Technology, Taipei Medical University, Taipei, Taiwan

PhD Program for Cancer Molecular Biology and Drug Discovery, College of Medical Science and Technology, Taipei Medical University, Taipei, Taiwan

^{*}TMU Research Center of Cancer Translational Medicine, Taipei Medical University, Taipei, Taiwan

hTMU Research Center for Drug Discovery, Taipei Medical University, Taipei, Taiwan PhD Program in Drug Discovery and Development Industry, College of Pharmacy, Taipei Medical University, Taipei, Taiwan

¹Master Program in Clinical Genomics and Proteomics, College of Pharmacy, Taipei Medical University, Taipei, Taiwan

 $[\]dagger$ Electronic supplementary information (ESI) available: HPLC purity data, 1H NMR spectra and ^{13}C NMR spectra of compounds 1–4, 8–9, and 13–15. See DOI: https://doi.org/10.1039/d3ra06600b

 $[\]ddagger$ These authors contributed equally to this work.

RSC Advances Paper

followed by a Friedel-Crafts reaction.19 The common ground of these methodologies is the use of indole and pyridine derivatives as starting materials in the construction of the C-ring of ellipticine quinone (3). Naciuk et al. conducted substitution of isoquinolin-5,8-dione followed by cross dehydrogenative coupling to obtain an isomer of ellipticine quinone (3).20 This strategy of B-ring formation attracted our attention due to its unprecedented route to ellipticine quinone (3) and ellipticine (1). However, the regioselective substitution of isoquinolin-5,8dione would appear to hamper the synthesis of ellipticine (1), because isoquinolin-5,8-dione favors C7 substitution.²¹ Considering that the synthesis of ellipticine (1) and isoellipticine (2) started from different starting materials and through different synthetic pathways. This study was aimed to develop a convergent pathway to ellipticine (1) and isoellipticine (2), beginning with the same starting material. This benefits the simultaneous comparison of their biological activity in the same study. For instance, this study tested the enzymatic activity of 1 and 2 against myosin light chain kinase family member 4 (MYLK4), which is correlated to the development of acute myeloid leukemia. In addition, this feasible synthetic methodology could be applied to understand the structureactivity relationship of (iso)ellipticine analogues in further study.

Results and discussion

Chemistry

The synthesis of isoellipticine (2) is shown in Scheme 1. The reaction of isoquinolin-5-ol (5) with [bis(trifluoroacetoxy)iodo] benzene (PIFA) followed by the addition of aniline generated predominantly compound 6 together with trace amounts of its regioisomer (9). This regioselective substitution of isoquinolin-5,8-dione was also observed by Naciuk²⁰ and Shin.²² Following reported methodology, isoellipticine quinone (4) was converted into isoellipticine (2).^{16,20} In comparison with Naciuk's work, this pathway is expeditious, generating isoellipticine (2) in four steps with a 19% overall yield.

Due to the predominant selective C7 substitution of isoquinolin-5,8-dione, an alternative synthetic route is required to achieve C6 substitution. Halogen atoms and methoxy substituent are helpful in the regioselective substitution of (iso) quinolinediones. A trial reaction of 6-bromoisoquinolin-5,8dione with aniline failed to form the anticipated product (9). In 2016, Zhao et al. reported a methodology fulfilling regioselective amination of phenol, which encouraged us to reorder the synthetic sequence.23 We tried to obtain 6-(phenylamino) isoquinolin-5-ol (7) using Zhao's methodology, and then to oxidize 7 to obtain 6-(phenylamino)isoquinoline-5,8-dione (9, Scheme 2). Interestingly, the reaction of isoquinolin-5-ol (5) with aniline in the presence of potassium persulfate (K₂S₂O₈) under the irradiation of blue light gave unexpectedly a p-iminoquinone (8) containing two anilino moieties as judged by NMR and mass spectra. We hydrolyzed 8 with acetic acid and H₂O²⁴ under reflux, yielding the anticipated compound (9). This result revealed that one aniline group had indeed been introduced at C6 of the isoquinoline-5,8-dione, and p-iminoquinone

Scheme 1 Synthetic approaches to isoellipticine (2): (a) (i) PIFA, EtOH/THF, H_2O , 0 °C to room temperature (rt); (ii) aniline, THF, rt; (b) $Pd(OAc)_2$, $Cu(OAc)_2$, PivOH, K_2CO_3 , DMA, 130 °C in a sealed tube; (c) (i) CH_3Li , tetramethylethylenediamine (TMEDA), sealed tube, THF, 0 °C to 100 °C; (ii) $NaBH_4$, EtOH, reflux.

Scheme 2 Synthetic approaches to ellipticine (1): (a) aniline, $K_2S_2O_8$, CH_3CN , 24W blue LED, rt; or conditions shown in Table 1; (b) glacial acetic acid, H_2O , reflux; (c) $Pd(OAc)_2$, $Cu(OAc)_2$, PivOH, K_2CO_3 , DMA, 130 °C in sealed tube; (d) (i) CH_3Li , TMEDA, sealed tube, THF, 0 °C to 100 °C; (ii) $NaBH_4$, EtOH, reflux.



Fig. 2 Key HMBC and NOESY interactions of p-iminoquinone (8).

(8) was the product of the $K_2S_2O_8$ -mediated reaction. Heteronuclear Multiple Bond Coherence (HMBC) and Nuclear Overhauser Effect Spectroscopy (NOESY) experiments were conducted to confirm the structure of the proposed p-iminoquinone (8), specifically the position of the imine moiety (Fig. 2

Table 1 Optimization and control experiments

Entry	Conditions	Additive	Time	Yield
1	Aniline (2 equiv.), persulfate (3 equiv.), rt, blue LED	_	64 h	4.5%
2	Aniline (20 equiv.), persulfate (3 equiv.), rt, blue LED	_	40 h	12.5%
3	Aniline (2 equiv.), persulfate (3 equiv.), rt, in the dark	_	64 h	2.1%
4	Aniline (1 equiv.), persulfate (3 equiv.), rt, in the dark	$TEMPO^a$	24 h	0
5	Aniline (1 equiv.), persulfate (3 equiv.), rt, in the dark	BQ^b	24 h	0
6	Aniline (1 equiv.), persulfate (3 equiv.), rt, in the dark	BHT^c	24 h	0
7	Aniline (10 equiv.), persulfate (3 equiv.), reflux	_	1 h	10.2%
8	Aniline (10 equiv.), persulfate (6 equiv.), reflux	_	1 h	19.2%

^a TEMPO: 2,2,6,6-tetramethyl-1-piperidinyloxy. ^b BQ: benzoquinone. ^c BHT: butylated hydroxytoluene.

and ESI†). The proton at $\delta_{\rm H}$ 9.81 ppm (H-1) in the NMR spectrum of 8 showed correlation with the 13 C-NMR spectra reported by Pradhan *et al.*²⁵ with a 13 C-NMR signal at $\delta_{\rm C}$ 154.10 ppm which is from the carbon atom (C-8) of the imine moiety. Correlations between the carbonyl carbon at $\delta_{\rm C}$ 181.56 ppm (C-6) and protons at $\delta_{\rm H}$ 7.96 ppm (H-4) signified the existence of a C=O group at the C-6 position. The quinone proton signal in 8 at $\delta_{\rm H}$ 6.72 ppm displayed NOESY signals between H-2′ and H-2′ ′. This result revealed that this quinone proton is H-7 and is located between the two phenyl moieties. Together with the results of hydrolysis product, HMBC and NOESY, we concluded that the $K_2S_2O_8$ -mediated reaction generated the *p*-iminoquinone (8). The following Pd-catalyzed cyclization converted compound 9 to the ellipticine quinone (3), which was subjected to reaction with CH₃Li and then NaBH₄ to generate ellipticine (1).

The scope and mechanism of the unexpected generation of *p*-iminoquinone (8) attracted our attention and we conducted the experiments shown in Table 1. Results from entries 1 and 3 in Table 1 indicated that this reaction proceeds independently of visible light. The increase of equivalence of aniline resulted in an increase in the reaction yield (entry 2). No conversion was observed in the presence of free radical scavengers such as TEMPO, BHT and benzoquinone (entries 4–6), which suggests a free radical mechanism for the formation of 8. In thermal reaction conditions the reaction time is dramatically shortened (entries 7 and 8), and 8 was obtained in a reaction time of 1 h, indicating that the reaction can be conducted through either a photo- or thermal-mediated pathway.

Pradhan *et al.* reported the synthesis of *p*-iminoquinone using nitrosobenzene in the presence of hexafluoroisopropanol (HFIP).²⁵ This study led us to examine the reaction of aniline with $K_2S_2O_8$ in the absence of isoquinolin-5-ol (5). This reaction failed to generate nitrosobenzene, revealing the involvement of a pathway different from the route proposed by Pradhan *et al.* In light of the results in Table 1, a radical mechanism for the

generation of p-iminoquinone (8) was proposed and is shown in Scheme 3. The potassium persulfate was photochemically or thermally cleaved to generate the corresponding sulfate radical which subsequently converted 5 into the radical (A). The addition of an aniline molecule followed by loss of a single electron resulted in another radical (C). A second aniline molecule was introduced and the subsequent oxidation generated the p-iminoquinone (8).

In an attempt to understand the scope of the $K_2S_2O_8$ -mediated synthesis of p-iminoquinones, we selected three heterocyclic compounds (10–12) each bearing one –OH group attached to the carbon adjacent to the ring fusion bond. Under the reaction conditions (Table 1, entry 8), compounds 10–12 were converted into the corresponding p-iminoquinones (13–15, Table 2). The resulting products produce the corresponding quinone derivatives through acetic acid-mediated hydrolysis. This methodology is helpful for regioselective synthesis of anilinoquinones because the position of the –OH determines the regioselectivity. A survey of the literature showed that reaction of aniline with persulfate yields polyaniline, 26 which could explain the very low yield of the reaction.

Scheme 3 Plausible reaction mechanism.

Table 2 Substrate scope of other OH-bearing heterocycles (10-12)

Entry	Substrate	Product	Yield
1	OH 10	N 13	12%
2	OH N		14%
3	ОН Н	0 H N N N N N N N N N N N N N N N N N N	18%

Derivatives of (iso)ellipticine, such as 7-hydroxyisoellipticine and 9-methoxyellipticine, have been reported having AML activity. 27,28 According to data from Gene Expression Profiling Interactive Analysis (GEPIA) database (Fig. S1†),29 the expression of myosin light chain kinase family member 4 (MYLK4) is significantly higher in acute myeloid leukemia tissues (T) when compared to normal tissues (N) and is considered as a potential therapeutic target for treatment of AML. In addition, some (iso) ellipticine derivatives were reported displaying kinase inhibition,30,31 which encouraged us to examine the effect of compounds 1-4 on MYLK4 and AML cells. Table 3 shows the enzymatic activity of compounds 1-4 against MYLK4. The result revealed that ellipticine (1) and isoellipticine (2) showed marked MYLK4 inhibitory activity as compared with their synthetic precursors (3 and 4), with IC₅₀ values of 7.1 and 6.1 nM, respectively. Due to their distinct MYLK4 inhibitory activity, compounds 1 and 2 were tested for their cellular activity against MV-4-11 and MOLM-13 cells. Despite the appearance of comparable kinase activity of compounds 1 and 2, 1 showed better AML activity than 2. Ellipticine (1) inhibited the growth of MV-4-11 and MOLM-13 cells with IC₅₀ values of 1.19 and 1.0 μ M, respectively. These results suggested that (iso)ellipticine could pave ways to the development of MYLK4 inhibitors for the treatment of AML.

Table 3 MYLK4 inhibitory activity (IC50, nM) and AML cellular activity (IC50, μ M) of tested compounds

	MYLK4	Cellular activity		
Compound		MV-4-11	MOLM-13	
1	7.1	1.19 ± 0.18	1.00 ± 0.33	
2	6.1	4.18 ± 0.61	$\textbf{5.11} \pm \textbf{0.30}$	
3	477.6	_	_	
4	285.6	_	_	

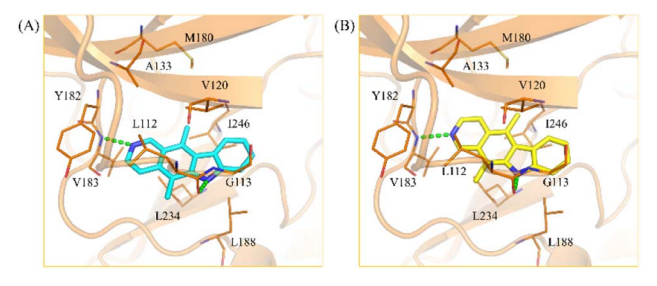


Fig. 3 Analysis of protein-ligand interactions. Docking poses of (A) compound 1 (blue) and (B) compound 2, (yellow) in the binding site of MYLK4 (orange). The pose suggests that the inhibitors occupy the targeted binding site. Hydrogen bonds are shown as green dashes. Binding site residues are labelled and displayed as lines.

Kinases contain a binding site pocket sandwiched by two lobes connected by a hinge loop.32 Incidentally, many kinase inhibitors targeting the binding site generate hydrogen bonds to the hinge loop residues.33 As a member of the human kinome, MYLK4 would contain similar features. Molecular docking was used to determine if the MYLK4 inhibitors in this study can favorably bind to MYLK4. The binding poses of 1 and 2 showed the occupation of areas associated with the adenosine ring of ATP. Both 1 and 2 were observed to form hydrogen bonds to V183 (Fig. 3). V183 forms part of the hinge loop, suggesting favorable occupation of the binding site. An additional hydrogen bond to the carbonyl backbone of residue L112 was also observed. These hydrogen bonds were facilitated by the nitrogen atoms present in the ring structures. The core structure of 1 and 2 provided more 'rigidity' to the compound and formed hydrophobic interactions with amino acids with aliphatic side chains, such as residues L112, V120, V183, L188, L234, and I246. Compound 2 generated additional hydrophobic interactions. This may be due to the location of its nitrogen atom as it formed a hydrogen bond to the hinge residue V183, which caused compound 2 to occupy a slightly different orientation toward residues G113, A133, and M180. This hydrophobic region also explains the distinct lose of MYLK4 activity of 3 and 4, due to appearance of two carbonyl groups. In addition, it guides the structural optimization by introducing hydrophobic substituents on A-ring in the future. Together, the docking results show favorable occupation of the MYLK4 binding site, and their interactions may facilitate their inhibitory activity.

Conclusions

This study attempted to provide pathways to ellipticine (1) and isoellipticine (2), starting from a common starting material. The modified four-step synthetic route provided isoellipticine (2) in 19% overall yield from compound 5. To address the problematic substitution of isoquinolin-5,8-dione, a $K_2S_2O_8$ -mediated *ortho*-amination was conducted and unexpectedly generated a *p*-iminoquinone (8) which could be converted into the ellipticine quinone (3) and further transformed to ellipticine (1). As a result, this study reported four-step synthetic routes to ellipticine (1) and isoellipticine (2). The $K_2S_2O_8$ -mediated synthesis

Paper

of *p*-iminoquinone was also studied for selected heterocycles 142.7, 140.6, 140.4

(10-12), revealing that the -OH group was able to direct substituents to its ortho position, thus providing an approach to address the issue of regioselective substitution of quinones. Given that biological activity of compounds 1 and 2 was discussed separately in the past, the achievement of this study is to fulfil comprehensive comparison of 1 and 2 as well as their synthetic precursors. The result revealed that (iso)ellipticine (1 and 2) displayed distinct inhibitory against MYLK4, which is highly expressed in acute myeloid leukemia tissues, as compared with (iso)ellipticine quinone (3 and 4). Despite of the appearance of comparable MYLK4 activity, compound 1 showed more potent AML activity than that of 2. Taken together, this study not only provided a regioselective methodology toward (iso)ellipticine (1 and 2) but also found 1 as a potential hit to develop MYLK4 inhibitors for AML treatment. In addition, our facile synthetic methodology would help us fulfil the structureactivity relationship study of (iso)ellipticine derivatives.

Experiment

Chemistry

Nuclear magnetic resonance spectra were obtained with an Agilent DD2 600 MHz NMR spectrometer operating at 600 MHz, with chemical shifts reported in parts per million (ppm, δ). High-resolution mass spectra (HRMS) were measured with a JEOL (JMS-700) electrospray ionization (ESI) mass spectrometer. The purity of the final compounds was determined using a Shimadzu LC-2030C LT and was found in all cases to be \geq 95%. Flash column chromatography was carried out using silica gel (Merck Kieselgel 60, no. 9385, 230–400 mesh ASTM). All reactions were conducted under an atmosphere of dry N₂.

5,11-Dimethyl-6H-pyrido[4,3-b]carbazole (1, ellipticine). A 2.2 M solution of CH₃Li in diethyl ether with LiBr (0.5 mL, 1.08 mmol) was added at 0 °C to a mixture of compound 3 (16.8 mg, 0.068 mmol), THF (10.2 mL), and TMEDA (0.33 mL, 2.17 mmol) in an argon-fluxed sealed tube. After the solution was stirred for 1 h, the reaction mixture was heated to 100 °C for 48 h. Then, the reaction mixture was cooled and a 2.2 M solution of CH₃Li in Et₂O with LiBr (0.5 mL, 1.08 mmol) was added at 0 °C. After the mixture was stirred at 100 °C for 26 h, the solvent was evaporated in vacuo. The crude product was dissolved in EtOH (30 mL) and NaBH₄ (0.31 g, 8.16 mmol) was added. The suspension was then stirred under reflux and NaBH₄ (0.15 g, 4.08 mmol) was added after 1 h. The reaction was cooled after 40 h, and the solvent was removed under vacuum. After the resulting solid was vigorously stirred with 26 mL of water and 17 mL of CHCl₃ for 3 h, the organic layer was separated. The aqueous layer was extracted with CHCl₃ and the organic phases were combined, dried by MgSO₄, and concentrated in vacuo. The residue was purified by flash column chromatography (DCM: MeOH = 95:5) on silica gel to give compound 1 as a yellow solid (8.1 mg, 48.4%). mp 281.7 °C (dec), ¹H NMR (600 MHz, DMSO- d_6) δ 11.37 (br, 1H), 9.70 (s, 1H), 8.43 (d, J = 6.0 Hz, 1H), 8.38 (d, J = 7.8 Hz, 1H), 7.92 (d, J = 6.0 Hz, 1H), 7.57 (d, J =8.4 Hz, 1H), 7.53 (t, J = 7.5 Hz, 1H), 7.26 (t, J = 7.5 Hz, 1H), 3.26 (s, 3H), 2.79 (s, 3H). ¹³C NMR (150 MHz, DMSO- d_6) δ 149.6,

142.7, 140.6, 140.4, 132.5, 128.0, 127.1, 123.8, 123.4, 123.1, 121.9, 119.2, 115.9, 110.7, 108.0, 14.3, 11.9. HRMS (ESI) for $C_{17}H_{15}N_2$ [M + H]⁺ calculated 247.1235, found 247.1236. HPLC purity: 99.7%.

5,11-Dimethyl-10*H*-pyrido[3,4-*b*]carbazole (2, isoellipticine). A 2.2 M solution of CH₃Li in Et₂O with LiBr (10.0 mL, 22 mmol) was added to a mixture of compound 4 (0.25 g, 1.01 mmol), THF (150.0 mL), and TMEDA (4.7 mL, 31.54 mmol) in an argonfluxed sealed tube at 0 °C. After stirring at 0 °C for 1 h, the reaction mixture was heated to 100 °C for 40 h. The solvent was evaporated in vacuo and the resulting crude product was dissolved in EtOH (440 mL) and NaBH₄ (4.49 g, 118.69 mmol) was added. The resulting suspension was heated to reflux and three additional batches of NaBH₄ (0.74 g each, 19.56 mmol) were added after 1, 6, and 23 h. The reaction mixture was cooled after 26 h, and the solvent was removed in vacuo. To the resulting residue was added H₂O (370 mL) and CHCl₃ (250 mL), and the mixture was vigorously stirred at rt for 20 h. The aqueous layer was extracted with CHCl3 and the organic phases were combined, dried by MgSO₄, and concentrated in vacuo. The residue was purified by flash column chromatography (DCM: MeOH = 95:5) on silica gel and washed with MeOH to give compound 2 as an yellow solid (80 mg, 32.1%). mp 257.5 °C (dec). 1 H NMR (600 MHz, DMSO- d_{6}) δ 11.35 (br, 1H), 9.59 (s, 1H), 8.41-8.40 (m, 2H), 8.13 (dd, J = 6.0, 0.6 Hz, 1H), 7.59-7.54(m, 2H), 7.25 (td, J = 7.2, 1.2 Hz, 1H), 3.14 (s, 3H), 2.96 (s, 3H). 13 C NMR (150 MHz, DMSO- d_6) δ 148.7, 143.1, 138.4, 138.4, 128.2, 127.6, 125.7, 125.3, 124.8, 124.2, 122.6, 118.9, 116.8, 110.7, 110.6, 14.5, 11.8. HRMS (ESI) for $C_{17}H_{15}N_2$ [M + H] calculated 247.1235, found 247.1237. HPLC purity: 97.9%.

5H-Pyrido[3,4-b]carbazole-5,11(6H)-dione (3). A mixture of compound 9 (0.13 g, 0.5 mmol), pivalic acid (0.46 g, 4.53 mmol), K_2CO_3 (20.7 mg, 30.0 mol%), $Pd(OAc)_2$ (33.7 mg, 30 mol%), Cu(OAc)₂ (0.27 g, 1.51 mmol), and DMA (10.0 mL) was placed in a sealed tube and heated at 130 °C for 30 h. The reaction mixture was filtered through Celite and washed with EtOAc. The filtrate was washed with an aqueous solution of NH₄OH/NH₄Cl (pH = 9), dried over MgSO₄, and concentrated in vacuo. The residue was purified by flash column chromatography (Hex: EtOAc = 2:1) on silica gel and washed with EtOAc to give compound 3 as an orange solid (15 mg, 12.1%). mp 336.8 °C (dec), ¹H NMR (600 MHz, DMSO- d_6) δ 13.21 (br, 1H), 9.25 (s, 1H), 9.07 (d, J = 4.8 Hz, 1H), 8.21 (d, J = 8.4 Hz, 1H), 7.93 (d, J =4.8 Hz, 1H), 7.61 (d, J = 8.4 Hz, 1H), 7.49–7.47 (m, 1H), 7.39 (td, J= 7.5, 0.6 Hz, 1H). 13 C NMR (150 MHz, DMSO- d_6) δ 180.2, 176.8, 155.1, 147.4, 138.5, 138.4, 136.8, 127.5, 126.5, 124.3, 123.6, 122.4, 118.3, 117.4, 113.9. HRMS (ESI) for $C_{15}H_9N_2O_2$ [M + H] calculated 249.0664, found 249.0664. HPLC purity: 89.7%.

5H-Pyrido[3,4-*b*]carbazole-5,11(10*H*)-dione (4). A mixture of compound **6** (0.69 g, 2.75 mmol), pivalic acid (2.52 g, 24.74 mmol), K_2CO_3 (0.11 g, 30.0 mol%), $Pd(OAc)_2$ (0.18 g, 30 mol%), $Cu(OAc)_2$ (1.50 g, 8.25 mmol), and DMA (55.0 mL) was placed in a sealed tube and heated at 130 °C for 40 h. The reaction mixture was filtered through Celite and washed with EtOAc. The filtrate was washed with an aqueous solution of NH_4OH/NH_4Cl (pH = 9), dried by MgSO₄, and concentrated *in vacuo*. The residue was purified by flash column chromatography (Hex:

EtOAc = 1.5:1) on silica gel and washed with MeOH to give compound 4 as an orange solid (0.19 g, 27.9%). mp 311.3–313.3 °C. ¹H NMR (600 MHz, DMSO- d_6) δ 13.23 (br, 1H), 9.22 (s, 1H), 9.08 (d, J = 4.4 Hz, 1H), 8.19 (d, J = 7.8 Hz, 1H), 7.95 (d, J = 4.8 Hz, 1H), 7.61 (d, J = 8.4 Hz, 1H), 7.47 (t, J = 7.5 Hz, 1H), 7.39 (t, J = 7.5 Hz, 1H). 13 C NMR (150 MHz, DMSO- d_6) δ 179.2, 177.2, 155.9, 147.1, 139.7, 138.2, 137.0, 127.3, 125.9, 124.4, 123.7, 122.3, 118.7, 117.5, 114.0. HRMS (ESI) for C₁₅H₉N₂O₂ [M + H]⁺ calculated 249.0664, found 249.0667. HPLC purity: 99.4% (a 7.4:1 mixture of regioisomers).

7-(Phenylamino)isoquinoline-5,8-dione (6). Compound 5 (1.20 g, 8.27 mmol) was added portionwise at 0 °C to [bis(trifluoroacetoxy)iodo]benzene (PIFA, 5.33 g, 12.40 mmol) in a 2:1 THF-H₂O solution (24 mL). After stirring at 0 °C for 2 h, aniline (0.60 mL, 6.57 mmol) was added to the resulting mixture at 0 °C. After stirring at rt for 18 h, the mixture was diluted with DCM and stirred at rt for 0.5 h. The resulting mixture was neutralized with saturated aqueous NaHCO3 solution and filtered through Celite. The filtrate was extracted with DCM, dried by MgSO₄, and concentrated in vacuo. The residue was purified by flash column chromatography (Hex: EtOAc = 4:1) on silica gel to give compound 6 as a red solid (0.45 g, 21.7%), mp 216.7-218.3 °C, ¹H NMR (600 MHz, DMSO- d_6) δ 9.47 (br, 1H), 9.20 (d, J = 0.6 Hz, 1H), 9.06 (d, J = 4.8 Hz, 1H), 7.81 (dd, J =4.9, 0.8 Hz, 1H), 7.48-7.45 (m, 2H), 7.39 (dd, J = 8.4, 1.2 Hz, 2H), 7.27-7.24 (m, 1H), 6.15 (s, 1H). 13 C NMR (150 MHz, DMSO- d_6) δ 181.1, 181.1, 156.0, 147.2, 146.6, 138.1, 137.6, 129.3, 125.7, 124.5, 124.0, 118.1, 102.1. HRMS (ESI) for $C_{15}H_{11}N_2O_2 [M + H]^{\dagger}$ calculated 251.0821, found 251.0822. HPLC purity: 97.5% (a 14.5:1 mixture of regioisomers).

(E)-6-(Phenylamino)-8-(phenylimino)isoquinolin-5(8H)-one (8). A mixture of isoquinolin-5-ol (5, 0.58 g, 4.00 mmol), $K_2S_2O_8$ (0.96 g, 23.97 mmol), aniline (3.76 g, 40.37 mmol), and MeCN (40 mL) was heated to reflux for 1 h. The reaction mixture was then filtered through Celite and washed with DCM. The filtrate was purified by flash column chromatography (Hex: EtOAc = 3:1) on silica gel and washed with EtOH to give compound 8 as a red solid (0.26 g, 20%). mp 228.0-228.8 °C, ¹H NMR (600 MHz, $CDCl_3$) δ 9.81 (d, J = 0.6 Hz, 1H), 8.94 (d, J = 5.4 Hz, 1H), 7.96 (dd, J = 5.1, 0.9 Hz, 1H), 7.38-7.36 (m, 2H), 7.29-7.26 (m, 3H),7.14-7.12 (m, 1H), 7.08-7.04 (m, 3H), 6.92 (dd, J = 8.1, 0.9 Hz, 2H), 6.72 (s, 1H). 13 C NMR (150 MHz, CDCl₃) δ 181.6, 154.1, 151.8, 150.9, 148.7, 140.4, 138.3, 135.2, 129.8, 129.1, 128.5, 124.9, 124.8, 121.4, 120.9, 118.0, 97.8. HRMS (ESI) for $C_{21}H_{16}N_3O[M+H]^+$ calculated 326.1293, found 326.1296. HPLC purity: 99.2%.

6-(Phenylamino)isoquinoline-5,8-dione (9). A mixture of compound 8 (0.40 g, 1.23 mmol), H₂O (4.0 mL), and AcOH (32.0 mL) was heated to reflux for 2.5 h. The reaction mixture was cooled and the solvent was evaporated *in vacuo*. The residue was purified by flash column chromatography (Hex: EtOAc = 2:1) on silica gel and washed with EtOH to give compound 9 as a dark red solid (0.19 g, 61.7%). mp 239.6–240.3 °C, ¹H NMR (600 MHz, DMSO- d_6) δ 9.37 (br, 1H), 9.13 (s, 1H), 9.04 (d, J = 5.4 Hz, 1H), 7.89 (d, J = 4.8 Hz, 1H), 7.47–7.45 (m, 2H), 7.39 (d, J = 7.2 Hz, 2H), 7.24 (t, J = 7.5 Hz, 1H), 6.10 (s, 1H). ¹³C NMR (150 MHz, DMSO- d_6) δ 182.2, 181.4, 154.3, 146.9, 146.5, 137.8, 136.1,

129.3, 125.5, 124.8, 123.8, 118.0, 102.0. HRMS (ESI) for $C_{15}H_{11}N_2O_2$ [M + H] $^+$ calculated 251.0821, found 251.0823. HPLC purity: 99.9%.

(*E*)-7-(Phenylamino)-5-(phenylimino)quinolin-8(5*H*)-one (13). The title compound was obtained in 12% overall yield from compound 10 in a manner similar to that described for the preparation of compound 8: 1 H NMR (600 MHz, CDCl₃) δ 8.99 (d, J = 3.0 Hz, 1H), 8.91 (d, J = 7.8 Hz, 1H), 7.67 (dd, J = 7.8, 4.2 Hz, 1H), 7.46 (s, 1H), 7.39 (t, J = 7.8 Hz, 2H), 7.29 (t, J = 7.8 Hz, 2H), 7.16–7.05 (m, 4H), 6.93 (d, J = 7.8 Hz, 1H), 6.74 (s, 1H). 13 C NMR (125 MHz, CDCl₃) δ 180.5, 154.0, 152.4, 150.9, 146.0, 140.9, 138.4, 134.1, 133.1, 129.6, 129.0, 127.4, 124.8, 124.6, 121.3, 120.8, 97.1. HRMS (ESI) for C₂₁H₁₆N₃O [M + H]⁺ calculated 326.1293, found 326.1282. HPLC purity: 95.3%.

(*E*)-5-(Phenylamino)-7-(phenylimino)-1,7-dihydro-4*H*-indol-4-one (14). The title compound was obtained in 14% overall yield from compound 11 in a manner similar to that described for the preparation of 8: 1 H NMR (600 MHz, DMSO- d_6) δ 12.45 (s, 1H), 8.47 (s, 1H), 7.38–7.34 (m, 2H), 7.27–7.23 (m, 2H), 7.21 (dd, J = 8.4, 1.2 Hz, 2H), 7.09 (tt, J = 7.2, 1.2 Hz, 1H), 7.06 7.21 (d, J = 3.0 Hz, 1H), 7.00 (tt, J = 7.2, 1.2 Hz, 1H), 6.94 (dd, J = 8.4, 1.2 Hz, 2H), 6.59 (d, J = 3.0 Hz, 1H), 5.98 (s, 1H). 13 C NMR (125 MHz, CDCl₃) δ 178.3, 151.6, 150.0, 141.7, 139.1, 136.5, 129.5, 129.0, 124.8, 124.1, 122.5, 121.7, 121.1, 120.4, 107.4, 91.8. HRMS (ESI) for $C_{20}H_{16}N_3O$ [M + H]⁺ calculated 314.1293, found 314.1282. HPLC purity: 97.1%.

(*E*)-3-(Phenylamino)-1-(phenylimino)-1,9-dihydro-4*H*-carbazol-4-one (15). The title compound was obtained in 18% overall yield from compound 12 in a manner similar to that described for the preparation of 8: 1 H NMR (600 MHz, DMSO- d_6) δ 12.79 (s, 1H), 8.69 (s, 1H), 8.11 (d, J = 1.8 Hz, 1H), 7.58 (d, J = 7.8 Hz, 1H), 7.42–7.39 (m, 2H), 7.37–33 (m, 1H), 7.33–7.25 (m, 5H), 7.13 (tt, J = 7.8 Hz, 1H), 7.06–7.01 (m, 3H), 6.06 (s, 1H). 13 C NMR (125 MHz, CDCl₃) δ 177.8, 151.8, 149.9, 142.8, 142.3, 139.0, 136.5, 129.6, 129.0, 125.4, 125.0, 125.0, 124.3, 123.5, 122.2, 121.6, 121.3, 112.6, 112.4, 91.2. HRMS (ESI) for C₂₄H₁₈N₃O [M + H]⁺ calculated 364.1450, found 364.1436. HPLC purity: 99.8%.

Cytotoxicity analysis

The cell viability was analyzed by MTT assay. MV-4-11 and MOLM-13 cells were seeded into 24-well plates at a density of 2 \times 105 cells per well and subsequently treated with the specified concentrations of compounds for a duration of 72 hours. Following treatment, MTT reagent (0.5 mg mL $^{-1}$ in PBS) was added and allowed to incubate with the cells for 1 hour. The resulting crystal formazan dyes were then dissolved in 1 mL of sodium acetate buffer (10% SDS with 0.01 N HCl). The absorbance was determined spectrophotometrically at 550 nm using an ELISA reader (Synergy HTX ELISA reader, Biotek, CA, USA). The IC $_{50}$ values of the compounds were calculated as the mean \pm standard deviation (SD).

Computational study

The MYLK4 protein structure (PDB ID: 2X4F) was downloaded from the Protein Data Bank repository.³⁴ Structures of the protein and small molecules were prepared with default

RSC Advances

settings using LeadIT (LeadIT version 2.2.0; BioSolveIT GmbH, https://www.biosolveit.de/LeadIT). This includes the removal of water molecules and the addition of hydrogen atoms. The active binding site was designated with a radius of 10 Å with the cocrystal ligand as the centroid. Molecular docking was performed within the LeadIT software suite. The number of solutions for fragmentation and iteration was set to 300. All other settings were set to default. Protein-ligand interactions were generated using Pipeline Pilot35 and rendered using PyMOL.

Conflicts of interest

There are no conflicts to declare.

Acknowledgements

This research was supported by the National Science and Technology Council, Taiwan (grant no. MOST111-2320-B-038-046 and NSTC 112-2320-B-110-002-MY3).

References

This article is licensed under a Creative Commons Attribution-NonCommercial 3.0 Unported Licence.

Open Access Article. Published on 30 October 2023. Downloaded on 12/4/2025 9:23:37 PM.

- 1 S. Goodwin, A. F. Smith and E. C. Horning, J. Am. Chem. Soc., 1959, 81, 1903.
- 2 D. Thompson, C. Miller and F. O. McCarthy, *Biochemistry*, 2008, 47, 10333-10344.
- 3 M. Stiborová, J. Poljaková, E. Martínková, J. Ulrichová, V. Simánek, Z. Dvořák and E. Frei, Toxicology, 2012, 302, 233-241.
- 4 E. C. O'Sullivan, C. M. Miller, F. M. Deane and F. O. McCarthy, Stud. Nat. Prod. Chem., 2013, 39, 189-232.
- 5 S. Miyake, A. Sasaki, T. Ohta and K. Shudo, Tetrahedron Lett., 1985, 26, 5815-5818.
- 6 C. Y. Liu and P. Knochel, J. Org. Chem., 2007, 72, 7106-7115.
- 7 S. Rasheed, D. N. Rao and P. Das, Asian J. Org. Chem., 2016, 5, 1499-1507.
- 8 G. W. Gribble, M. G. Saulnier, M. P. Sibi and J. A. Obaza-Nutaitis, J. Org. Chem., 1984, 49, 4518-4523.
- 9 D. A. Davis and G. W. Gribble, Tetrahedron Lett., 1990, 31,
- 10 C. May and C. J. Moody, J. Chem. Soc., Perkin Trans. 1, 1988, 2, 247-250.
- 11 P. A. Cranwell and J. E. Saxton, J. Chem. Soc., 1962, 3482-3487.
- 12 L. K. Dalton, S. Demerac, B. C. Elmes, J. W. Loder, J. M. Swan and T. Teitei, Aust. J. Chem., 1967, 20, 2715-2727.
- 13 H. Y. Lee, G. S. Chen, C. S. Chen and J. W. Chern, J. Heterocycl. Chem., 2010, 47, 454-458.
- 14 E. Differding and L. Ghosez, Tetrahedron Lett., 1985, 26, 1647-1650.

- 15 J. M. Pedersen, W. R. Bowman, M. R. Elsegood, A. J. Fletcher and P. J. Lovell, J. Org. Chem., 2005, 70, 10615-10618.
- 16 M. G. Saulnier and G. W. Gribble, J. Org. Chem., 1983, 48, 2690-2695.
- 17 M. Watanabe and V. Snieckus, J. Am. Chem. Soc., 1980, 102, 1457-1460.
- 18 N. Ramkumar and R. Nagarajan, J. Org. Chem., 2014, 79, 736-
- 19 D. H. Dethe and G. M. Murhade, Eur. J. Org Chem., 2014,
- 20 F. F. Naciuk, J. A. M. Castro, B. K. Serikava and P. C. M. L. Miranda, ChemistrySelect, 2018, 3, 436-439.
- 21 F. F. Naciuk, J. C. Milan, A. Andreão and P. C. M. L. Miranda, J. Org. Chem., 2013, 78, 5026-5030.
- 22 N. N. Shin, H. Jeon, Y. Jung, S. Baek, S. Lee, H. C. Yoo, G. H. Bae, K. Park, S. H. Yang, J. M. Han, I. Kim and Y. Kim, ACS Chem. Neurosci., 2019, 10, 3031-3044.
- 23 Y. Zhao, B. Huang, C. Yang and W. Xia, Org. Lett., 2016, 18, 3326-3329.
- 24 L. M. Gornostaev, T. A. Rukovets, T. I. Lavrikova, Y. G. Khalyavina and G. A. Stashina, Russ. Chem. Bull., 2017, 66, 1007-1010.
- 25 S. Pradhan, S. Roy, S. Ghosh and I. Chatterjee, Adv. Synth. Catal., 2019, 361, 4294-4301.
- 26 I. Y. Sapurina and M. A. Shishov, Intech, 1989, 32, 137-144.
- 27 E. G. Russell, E. C. O'Sullivan, C. M. Miller, J. Stanicka, F. O. McCarthy and T. G. Cotter, Invest. New Drugs, 2014, 32, 1113-1122.
- 28 B. M. Ansari and E. N. Thompson, Postgrad. Med. J., 1975, 51, 103-105.
- 29 Z. Tang, C. Li, B. Kang, G. Gao, C. Li and Z. Zhang, Nucleic Acids Res., 2017, 45, W98-W102.
- 30 X. Jin, D. R. Gossett, S. Wang, D. Yang, Y. Cao, J. Chen, R. Guo, R. K. Reynolds and J. Lin, Br. J. Cancer, 2004, 91, 1808-1812.
- 31 J. Vendôme, S. Letard, F. Martin, F. Svinarchuk, P. Dubreuil, C. Auclair and M. Le Bret, J. Med. Chem., 2005, 48, 6194-6201.
- 32 M. M. Attwood, D. Fabbro, A. V. Sokolov, S. Knapp and H. B. Schiöth, Nat. Rev. Drug Discovery, 2021, 20, 839-861.
- 33 Z. S. Derewenda, I. Hawro and U. Derewenda, IUBMB Life, 2020, 72, 1233-1242.
- 34 P. D. B. C. ww, Protein Data Bank: the single global archive for 3D macromolecular structure data, Nucleic Acids Res., 2019, 47, D520-D528, DOI: 10.1093/nar/gky949.
- 35 Dassault Systèmes BIOVIA Pipeline Pilot, Release 2017, Dassault Systemes, San Diego.